

Synthesis of Zinc Hydrazonide Complexes

Saba Javed and David M. Hoffman*

Department of Chemistry, University of Houston, Houston, Texas 77204-5003

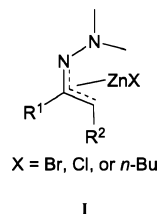
Received August 1, 2008

The zinc hydrazonide complexes $[\text{ClZn}(\text{CH}_2\text{C}(\text{Me})=\text{NNMe}_2)(\text{py})_2]$, $[\text{ClZn}(\text{CH}_2\text{C}(t\text{-Bu})=\text{NNMe}_2)_2]$, $[\text{Zn}(\text{CH}_2\text{C}(\text{Me})=\text{NNMe}_2)_2]_2$, $[\text{Zn}(\text{CH}_2\text{C}(i\text{-Pr})=\text{NNMe}_2)_2]$, and $[\text{Zn}(\text{CH}_2\text{C}(t\text{-Bu})=\text{NNMe}_2)_2]$ were synthesized by salt metathesis reactions, and the coordination polymer $[\text{EtZn}(\text{CH}_2\text{C}(\text{Me})=\text{NNMe}_2)]_n$ was obtained from the reaction between excess ZnEt_2 and $[\text{Zn}(\text{CH}_2\text{C}(\text{Me})=\text{NNMe}_2)_2]_2$. Single crystal X-ray crystallography studies revealed that the hydrazonide ligands were bound to zinc as chelating alkyl ligands. The ligand precursor $[\text{Li}(\text{CH}_2\text{C}(i\text{-Pr})=\text{NNMe}_2)(\text{THF})]_n$ was also structurally characterized. In the anion of $[\text{Li}(\text{CH}_2\text{C}(i\text{-Pr})=\text{NNMe}_2)(\text{THF})]_n$, the hydrazonide ligand in $[\text{EtZn}(\text{CH}_2\text{C}(\text{Me})=\text{NNMe}_2)]_n$, and the bridging hydrazonide ligands in $[\text{Zn}(\text{CH}_2\text{C}(\text{Me})=\text{NNMe}_2)_2]_2$ and $[\text{ClZn}(\text{CH}_2\text{C}(\text{Me})=\text{NNMe}_2)(\text{py})_2]$, there is evidence for three-center charge delocalization. In solution, the dimer $[\text{Zn}(\text{CH}_2\text{C}(\text{Me})=\text{NNMe}_2)_2]_2$ is in equilibrium with the monomer $\text{Zn}(\text{CH}_2\text{C}(\text{Me})=\text{NNMe}_2)_2$. The thermodynamic parameters $\Delta H^\circ = 55.8(2.9)$ kJ/mol, $\Delta S^\circ = 144(2)$ J/mol K, and $\Delta G^\circ_{298\text{K}} = 13(2)$ kJ/mol for the equilibrium were obtained from a variable temperature ^1H NMR study.

Introduction

In a series of papers, Nakamura and co-workers reported new C–C bond forming reactions involving proposed zinc hydrazonide intermediates (**I**).^{1–3} In their proposed scheme, they formed zinc hydrazonide intermediates in situ from zinc halides and lithium hydrazonides, and the proposed zinc hydrazonide intermediates reacted under mild conditions with olefins, including ethylene, via insertion into the Zn–C bonds. Subsequent quenching of the insertion products with electrophiles yielded the final organic products. In these studies, none of the organometallic zinc intermediates was isolated.

On the basis of the proposal by Nakamura et al. that zinc hydrazonides readily insert olefins, we set out to synthesize zinc hydrazonide complexes and determine whether the isolated complexes showed similar olefin insertion chemistry and if so, whether they could be activated for olefin polymerization. We report here on our initial synthetic studies, which include the isolation and characterization of



homoleptic zinc hydrazonide complexes, zinc hydrazonide alkyl complexes, and zinc hydrazonide chlorido complexes.

Experimental Section

General Procedures and Reagents. All manipulations were carried out in a glovebox or by using Schlenk techniques. The solvents were purified according to standard methods and stored in the glovebox over molecular sieves. 3-Methyl-2-butanone, 3,3-dimethyl-2-butanone, MgSO_4 , CaH_2 , ZnEt_2 and 1,1-dimethylhydrazine were purchased from Aldrich, and ZnCl_2 was purchased from Strem. The hydrazone $\text{Me}_2\text{C}=\text{NNMe}_2$ was prepared according to a literature method,^{4,5} and the hydrazones $\text{Me}(i\text{-Pr})\text{C}=\text{NNMe}_2$ and $\text{Me}(t\text{-Bu})\text{C}=\text{NNMe}_2$ were synthesized by using a slightly modified version of published procedures, as described below.^{6–8}

Proton and ^{13}C NMR spectra were referenced internally to solvent proton and carbon-13 resonances, respectively. Nuclear magnetic

* To whom correspondence should be addressed. E-mail: hoffman@uh.edu.

- (1) Kubota, K.; Nakamura, E. *Angew. Chem., Int. Ed. Engl.* **1997**, *36*, 2491.
- (2) Nakamura, E.; Kubota, K.; Sakata, G. *J. Am. Chem. Soc.* **1997**, *119*, 5457.
- (3) Nakamura, M.; Hara, K.; Sakata, G.; Nakamura, E. *Org. Lett.* **1999**, *1*, 1505.

- (4) Lehn, J.-S. Ph. D. Thesis, University of Houston, 2005; page 112.
- (5) Corey, E. J.; Enders, D. *Chem. Ber.* **1978**, *111*, 1337.
- (6) Sharma, S. D.; Pandhi, S. B. *J. Org. Chem.* **1990**, *55*, 2196.
- (7) Karabatsos, G. J.; Taller, R. A. *Tetrahedron* **1968**, *24*, 3923.
- (8) Smith, P. A. S.; Most, E. E., Jr. *J. Org. Chem.* **1957**, *22*, 358.

resonance spectra were recorded on a 300-MHz instrument unless noted otherwise. Infrared data were collected neat or as Nujol mulls between NaCl or KBr plates. Midwest Microlab, Indianapolis, IN, performed the elemental analysis.

Me(*i*-Pr)C=NNMe₂. In a round-bottom flask, 1,1-dimethylhydrazine (25.0 g, 416 mmol) was added to cold (0 °C) 3-methyl-2-butanone (32.5 g, 378 mmol). The solution was warmed to room temperature and refluxed (12 h). After refluxing, the mixture was distilled, and the fraction distilling at >90 °C was collected. The distillate volume was increased by adding diethyl ether (50 mL). The resulting solution was washed with distilled water, dried over MgSO₄, and finally distilled under argon over CaH₂ (bp 95–98 °C/0.02 mmHg). The product was a colorless liquid (yield 35.7 g, 74%). *E* isomer (90%) ¹H NMR (C₆D₆): δ 0.99 (d, 6, *J* = 6 Hz, CH₃C(CH(CH₃)₂)=NN(CH₃)₂), 1.73 (s, 3, CH₃C(CH(CH₃)₂)=NN(CH₃)₂), 2.38 (sept, 1, *J* = 7 Hz, CH₃C(CH(CH₃)₂)=NN(CH₃)₂), 2.40 (s, 6, CH₃C(CH(CH₃)₂)=NN(CH₃)₂). ¹³C{¹H} NMR (C₆D₆): δ 14.1 (CH₃C(CH(CH₃)₂)=NN(CH₃)₂), 20.2 (CH₃C(CH(CH₃)₂)=NN(CH₃)₂), 37.0 ((CH₃C(CH(CH₃)₂)=NN(CH₃)₂)), 47.1 (CH₃C(CH(CH₃)₂)=NN(CH₃)₂), 170.0 (CH₃C(CH(CH₃)₂)=NN(CH₃)₂). *Z* isomer (10%) ¹H NMR (C₆D₆): Only two resonances were observed because of overlap of resonances with the *E* isomer. δ 0.82 (d, 6, *J* = 8 Hz, CH₃C(CH(CH₃)₂)=NN(CH₃)₂), 1.71 (s, 3, CH₃C(CH(CH₃)₂)=NN(CH₃)₂). IR (Nujol, NaCl, cm⁻¹): ν(C=N) 1632 s, 1198 m, 1144 m, 1099 m, 1077 m, 1021 m, 982 m, 959 m, 897 w, 834 w, 772 w, 595 w.

Me(*t*-Bu)C=NNMe₂. In a round-bottom flask, 1,1-dimethylhydrazine (27.0 g, 450 mmol) was added to cold (0 °C) 3,3-dimethyl-2-butanone (30.0 g, 300 mmol). The solution was warmed to room temperature and refluxed (12 h). After refluxing, the mixture was distilled, and the fraction distilling at >105 °C was collected. Diethyl ether was added to increase the distillate volume (50 mL). The resulting solution was washed with distilled water, dried over MgSO₄, and finally distilled under argon over CaH₂ (bp 105–110 °C/0.02 mmHg; lit. 130 °C/740 mmHg). The product was a colorless liquid (yield 35.1 g, 82%). ¹H NMR (C₆D₆): δ 1.08 (s, 9, CH₃C(C(CH₃)₃)=NN(CH₃)₂), 1.81 (s, 3, CH₃C(C(CH₃)₃)=NN(CH₃)₂), 2.39 (s, 6, CH₃C(C(CH₃)₃)=NN(CH₃)₂). ¹³C{¹H} NMR (C₆D₆): δ 12.2 (CH₃C(C(CH₃)₃)=NN(CH₃)₂), 28.3 (CH₃C(C(CH₃)₃)=NN(CH₃)₂), 38.2 (CH₃C(C(CH₃)₃)=NN(CH₃)₂), 47.1 (CH₃C(C(CH₃)₃)=NN(CH₃)₂), 171.8 (CH₃C(C(CH₃)₃)=NN(CH₃)₂). IR (Nujol, NaCl, cm⁻¹): ν(C=N) 1621 s, 1215 m, 1198 m, 1140 vs, 1088 w, 1037 m, 1021 m, 985 s, 956 m, 861 w, 822 vw, 736 w.

Li(CH₂C(*i*-Pr)=NNMe₂). A cold solution (–25 °C) of dry MeC(*i*-Pr)=NNMe₂ (10. g, 78 mmol) in hexanes (50 mL) was added slowly to a cold solution of *n*-butyl lithium (1.6 *M*, 49 mL, 78 mmol) in hexanes (20 mL). When the addition was completed, the mixture was allowed to warm to room temperature whereupon it was stirred for 12 h. The mixture was filtered over a glass frit. The white solid on the frit was washed with hexanes (3 × 50 mL) and then dried under vacuum (yield 8.7 g, 83%). The salt may be crystallized from tetrahydrofuran (THF), which produces the THF adduct; THF is partially lost from the adduct under vacuum. Anal. Calcd for C₇H₁₃LiN₂: C, 62.67; H, 11.27; N, 20.88. Found: C, 62.92; H, 11.19; N, 20.41. ¹H NMR (THF-*d*₈): δ 1.08 (d, 6, *J* = 7 Hz, CH₂C(CH(CH₃)₂)=NN(CH₃)₂), 1.92 (sept, 1, *J* = 7 Hz, CH₂C(CH(CH₃)₂)=NN(CH₃)₂), 2.31 (s, 1, CH₂C(CH(CH₃)₂)=NN(CH₃)₂), 2.42 (s, 6, CH₂C(CH(CH₃)₂)=NN(CH₃)₂). ¹³C{¹H} NMR (THF-*d*₈): δ 12.0 (CH₂C(CH(CH₃)₂)=NN(CH₃)₂), 18.3 (CH₂C(CH(CH₃)₂)=NN(CH₃)₂), 35.4 (CH₂C(CH(CH₃)₂)=NN(CH₃)₂), 45.1 (CH₂C(CH(CH₃)₂)=NN(CH₃)₂), 168.6 (CH₂C(CH(CH₃)₂)=NN(CH₃)₂). IR

(Nujol, NaCl, cm⁻¹): 3100 w, 2772 w, 1548 vs, 1304 m, 1265 s, 1220 w, 1201 w, 1163 m, 1109 w, 1082 s, 1015 s, 965 s, 914 w, 874 m, 790 w, 690 s, 605 m, 540 s.

The lithium salts Li(CH₂C(R)=NNMe₂) where R = Me and *t*-Bu were synthesized from the hydrazones and *n*-BuLi as described for Li(CH₂C(*i*-Pr)=NNMe₂).

[ClZn(CH₂C(*t*-Bu)=NNMe₂)₂], Li(CH₂C(*t*-Bu)=NNMe₂) (0.45 g, 3.0 mmol) was added to a suspension of ZnCl₂ (0.40 g, 3.0 mmol) in diethyl ether (25 mL). The mixture was stirred at room temperature for 12 h before the ether was removed under vacuum to yield a yellow powder. Pentane (2 × 20 mL) was added to the residue, and the mixture was filtered over Celite. The filtrate was evaporated under vacuum, and the resulting white powder was dissolved in the minimum amount of toluene. The flask was placed in the freezer for crystallization (–25 °C). After 24 h, colorless crystals were isolated (yield 0.49 g, 70%). Anal. Calcd for C₈H₁₇N₂ClZn: C, 39.69; H, 7.08; N, 11.57. Found: C, 39.50; H, 7.37; N, 11.47. ¹H NMR (C₆D₆): δ 1.17 (s, 2, CH₂C(C(CH₃)₃)=NN(CH₃)₂), 1.20 (s, 9, CH₂C(C(CH₃)₃)=NN(CH₃)₂), 2.38 (s, 6, CH₂C(C(CH₃)₃)=NN(CH₃)₂). ¹³C{¹H} NMR (C₆D₆): δ 8.7 (CH₂C(C(CH₃)₃)=NN(CH₃)₂), 28.4 (CH₂C(C(CH₃)₃)=NN(CH₃)₂), 39.8 (CH₂C(C(CH₃)₃)=NN(CH₃)₂), 47.4 (CH₂C(C(CH₃)₃)=NN(CH₃)₂), 188.3 (CH₂C(C(CH₃)₃)=NN(CH₃)₂). IR (neat, KBr, cm⁻¹): 3064 m, 3037 m, 2971 w, 2933 w, 2908 w, 2871 w, 2757 w, 1620 vs, 1468 s, 1434 m, 1397 w, 1369 m, 1333 w, 1235 w, 1177 m, 1144 w, 1041 w, 987 w, 903 s, 824 w, 707 s, 526 w.

[ClZn(CH₂C(Me)=NNMe₂)(py)]₂, Li(CH₂C(Me)=NNMe₂) (0.235 g, 2.21 mmol) was added to a suspension of ZnCl₂ (0.300 g, 2.21 mmol) in diethyl ether (25 mL). The mixture was stirred at room temperature for 12 h before the ether was removed under vacuum to yield a yellow powder. Benzene (3 × 20 mL) was added to the residue, and the resulting suspension was filtered over Celite. The filtrate was evaporated under vacuum, and toluene (2 mL) was added to the resulting white powder. Pyridine (3 drops) was added to the suspension in toluene to dissolve the precipitate. The volume was reduced in vacuo, and the flask was then placed in the glovebox freezer (–25 °C). After 12 h, colorless crystals had formed, which were isolated by decanting the mother liquor with a pipet (yield 0.43 g, 70%). Anal. Calcd for C₂₀H₃₂N₆Cl₂Zn₂: C, 43.03; H, 5.78; N, 15.06. Found: C, 43.19; H, 5.69; N, 15.20. NMR assignments are based on the assumption that a complex with a hydrazone ligand formed in solution (see text for discussion). ¹H NMR (THF-*d*₈): δ 2.37 (s, 3, N(NMe₂)(C(Me)=CH₂)), 2.63 (br, 6, N(NMe₂)(C(Me)=CH₂)), 3.51 (d, 1, ²*J* = 1.5 Hz, N(NMe₂)(C(Me)=CH₂)), 4.04 (d, 1, ²*J* = 1.5 Hz, N(NMe₂)(C(Me)=CH₂)), 7.48 (*m*-py), 7.89 (*p*-py), 8.70 (*o*-py). The ¹³C spectrum was assigned by using a ¹³C–¹H COSY (600 MHz) experiment. ¹³C{¹H} NMR (THF-*d*₈): δ 32.0 (N(NMe₂)(C(Me)=CH₂)), 46.2 (N(NMe₂)(C(Me)=CH₂)), 94.6 (N(NMe₂)(C(Me)=CH₂)), 124.7 (2, *m*-py), 138.4 (1, *p*-py), 149.0 (1, *o*-py), 190.9 (N(NMe₂)(C(Me)=CH₂)). IR (neat, NaCl, cm⁻¹): 1607 s, 1573 vw, 1558 vw, 1541 vw, 1487 w, 1448 vs, 1244 vw, 1217 w, 1159 w, 1069 m, 1044 m, 1016 w, 887 br, 797 br, 760 m, 751 w, 697 vs, 640 m, 522 m.

[Zn(CH₂C(Me)=NNMe₂)₂], Li(CH₂C(Me)=NNMe₂) (1.50 g, 14.1 mmol) was added to a suspension of ZnCl₂ (0.960 g, 7.07 mmol) in diethyl ether (30 mL). The mixture was stirred at room temperature for 12 h before the ether was removed under vacuum to yield a yellow powder. Pentane (2 × 20 mL) was added to the residue, and the mixture was filtered over Celite. The clear yellow filtrate was evaporated under vacuum, and the resulting yellow powder was dissolved in the minimum amount of toluene. The flask was placed in the freezer for crystallization (–25 °C). After 24 h, yellowish crystals were isolated. The crystalline product was

sublimed (70 °C, 0.01 mmHg) to yield a colorless solid on the coldfinger (yield 0.86 g, 46%). Anal. Calcd for $C_{10}H_{22}N_4Zn$: C, 45.55; H, 8.41; N, 21.25. Found: C, 45.26; H, 8.38; N, 21.06. Dimer (see text): 1H NMR (C_6D_6): δ 1.33 and 1.38 (d of an AB q, $J = 13$ Hz, 4, $CH_2C(CH_3)=NN(CH_3)_2$), 1.77 and 2.27 (d of an AB q, 4, $J = 4$ Hz, μ - $CH_2C(CH_3)=NN(CH_3)_2$), 2.05 and 2.21 (s, 6, $CH_2C(CH_3)=NN(CH_3)_2$), 2.34 (br, 12, $CH_2C(CH_3)=NN(CH_3)_2$), 2.47 (s, 6, $CH_2C(CH_3)=NN(CH_3)_2$), 2.53 (s, 6, $CH_2C(CH_3)=NN(CH_3)_2$). A ^{13}C - 1H COSY spectrum was used to assign C-13 chemical shifts. $^{13}C\{^1H\}$ NMR (C_6D_6): δ 20.90 ($CH_2C(CH_3)=NN(CH_3)_2$), 23.42 ($CH_2C(CH_3)=NN(CH_3)_2$), 27.32 ($CH_2C(CH_3)=NN(CH_3)_2$), 33.63 (μ - $CH_2C(CH_3)=NN(CH_3)_2$), 47.65 ($CH_2C(CH_3)=NN(CH_3)_2$), 47.99 ($CH_2C(CH_3)=NN(CH_3)_2$), 49.14 ($CH_2C(CH_3)=NN(CH_3)_2$), 180.11 ($CH_2C(CH_3)=NN(CH_3)_2$), 186.63 ($CH_2C(CH_3)=NN(CH_3)_2$). Monomer: 1H NMR (C_6D_6): δ 1.11 (s, 2, $CH_2C(CH_3)=NN(CH_3)_2$), 2.05 (s, 6, $CH_2C(CH_3)=NN(CH_3)_2$), 2.25 (s, 12, $CH_2C(CH_3)=NN(CH_3)_2$). A ^{13}C - 1H COSY spectrum was used to assign C-13 chemical shifts. $^{13}C\{^1H\}$ NMR (C_6D_6): δ 16.71 ($CH_2C(CH_3)=NN(CH_3)_2$), 26.79 ($CH_2C(CH_3)=NN(CH_3)_2$), 47.24 ($CH_2C(CH_3)=NN(CH_3)_2$), 179.95 ($CH_2C(CH_3)=NN(CH_3)_2$). IR (Nujol, NaCl, cm^{-1}): 3091 m, 3072 m, 3036 s, 2724 w, 1953 w, 1808 w, 1591 w, 1478 vs, 1304 w, 1169 w, 1154 w, 1036 m, 965 vw, 936 vw, 845 vw, 674 vs.

$Zn(CH_2C(i-Pr)=NNMe_2)_2$. This compound was synthesized following the method described for $[Zn(CH_2C(Me)=NNMe_2)_2]_2$. The product was sublimed (55 °C, 0.01 mmHg) to yield a colorless solid on the coldfinger (yield 48%). Anal. Calcd for $C_{14}H_{30}N_4Zn$: C, 52.58; H, 9.46; N, 17.52. Found: C, 52.37; H, 9.27; N, 17.47. 1H NMR (C_6D_6): δ 1.04 (s, 2, $CH_2C(CH(CH_3)_2)=NN(CH_3)_2$), 1.20 (d, 6, $J = 7$ Hz, $CH_2C(CH(CH_3)_2)=NN(CH_3)_2$), 2.27 (s, 6, $CH_2C(CH(CH_3)_2)=NN(CH_3)_2$), 2.67 (sept, 1, $J = 7$ Hz, $CH_2C(CH(CH_3)_2)=NN(CH_3)_2$). $^{13}C\{^1H\}$ NMR (C_6D_6): δ 11.68 ($CH_2C(CH(CH_3)_2)=NN(CH_3)_2$), 21.38 ($CH_2C(CH(CH_3)_2)=NN(CH_3)_2$), 38.43 ($CH_2C(CH(CH_3)_2)=NN(CH_3)_2$), 47.86 ($CH_2C(CH(CH_3)_2)=NN(CH_3)_2$), 187.30 ($CH_2C(CH(CH_3)_2)=NN(CH_3)_2$). IR (neat, NaCl, cm^{-1}): 1517 vs, 1474 vs, 1394 w, 1354 m, 1333 w, 1289 w, 1258 s, 1242 s, 1208 s, 1191 s, 1118 w, 1096 m, 1008 w, 939 w, 919 w, 891 w, 827 s, 759 s, 700 w, 690 w, 610 m, 517 m, 460 w, 439 w, 417 w.

$Zn(CH_2C(t-Bu)=NNMe_2)_2$. This compound was synthesized following the method described for $[Zn(CH_2C(Me)=NNMe_2)_2]_2$. The product was sublimed (75 °C, 0.01 mmHg) to yield a colorless solid on the coldfinger (64%). Anal. Calcd for $C_{16}H_{34}N_4Zn$: C, 55.24; H, 9.85; N, 16.11. Found: C, 54.92; H, 9.61; N, 16.02. 1H NMR (C_6D_6): δ 1.07 (s, 2, $CH_2C(C(CH_3)_3)=NN(CH_3)_2$), 1.29 (s, 9, $CH_2C(C(CH_3)_3)=NN(CH_3)_2$), 2.25 (s, 6, $CH_2C(C(CH_3)_3)=NN(CH_3)_2$). $^{13}C\{^1H\}$ NMR (C_6D_6): δ 10.4 ($CH_2C(C(CH_3)_3)=NN(CH_3)_2$), 29.6 ($CH_2C(C(CH_3)_3)=NN(CH_3)_2$), 40.1 ($CH_2C(C(CH_3)_3)=NN(CH_3)_2$), 48.0 ($CH_2C(C(CH_3)_3)=NN(CH_3)_2$), 189.1 ($CH_2C(C(CH_3)_3)=NN(CH_3)_2$). IR (neat, NaCl, cm^{-1}): 1557 s, 1507 m, 1456 w, 1397 vs, 1319 w, 1299 w, 1199 br, 1160 w, 1099 w, 1020 w, 824 w, 743 m, 579 w, 571 w, 506 w.

$[EtZn(CH_2C(Me)=NNMe_2)]_n$. $ZnEt_2$ (0.48 g, 3.9 mmol) was added to a solution of $[Zn(CH_2C(Me)=NNMe_2)_2]_2$ (0.10 g, 0.19 mmol) in diethyl ether (25 mL). The solution was stirred for 12 h before the ether was removed under vacuum. The solid residue was extracted with hexanes (2×30 mL) and filtered over a glass frit. The solid on the frit was dissolved in a minimum amount of THF (2 mL). The flask was placed in the freezer (-25 °C) for crystallization. Colorless crystals were isolated after 24 h by removing the mother liquor with a pipet (yield 0.082 g, 56%). Anal. Calcd for $C_7H_{16}N_2Zn$: C, 43.43; H, 8.33; N, 14.47. Found: C, 43.39; H, 8.01; N, 14.08. 1H NMR (THF- d_8): δ 0.11 (q, 2, $J = 8$ Hz,

$ZnCH_2CH_3$), 0.96 (s, 2, $CH_2C(Me)=NN(CH_3)_2$), 1.21 (t, 3, $J = 8$ Hz, $ZnCH_2CH_3$), 1.95 (s, 3, $ZnCH_2C(CH_3)=NN(CH_3)_2$), 2.48 (s, 6, $CH_2C(Me)=NN(CH_3)_2$). $^{13}C\{^1H\}$ NMR (THF- d_8): δ 12.6, 17.6 and 21.0 ($ZnCH_2C(CH_3)=NN(CH_3)_2$, $ZnCH_2CH_3$, and $ZnCH_2CH_3$), 26.5 ($ZnCH_2C(CH_3)=NN(CH_3)_2$), 47.3 ($ZnCH_2C(CH_3)=NN(CH_3)_2$), 180.0 ($ZnCH_2C(CH_3)=NN(CH_3)_2$). IR (neat, NaCl, cm^{-1}): 1700 w, 1654 w, 1547 s, 1508 w, 1418 m, 1396 vs, 1319 vw, 1289 vw, 1246 vw, 1161 vw, 1133 vw, 1103 vw, 1073 vw, 1043 vw, 1020 w, 979 w, 924 m, 901 m, 845 vw, 827 vw, 738 m, 659 vw, 609 vw, 573 w, 541 vw, 508 vw, 490 vw.

Dimer-Monomer Equilibrium Study. The equilibrium $[Zn(CH_2C(Me)=NNMe_2)_2]_2 \rightleftharpoons 2Zn(CH_2C(Me)=NNMe_2)_2$ was studied using 1H NMR spectroscopy. A solution with a known concentration of $[Zn(CH_2C(Me)=NNMe_2)_2]_2$ (0.050 g) and trichlorobenzene (0.034 g) in xylene- d_{10} (0.70 mL) was prepared in an NMR tube equipped with a Teflon stopcock. Data was collected at 0, 25, 40, 60, and 80 °C. At each temperature, the sample was allowed to equilibrate for at least 10 min before data were collected. To determine the absolute concentrations of $[Zn(CH_2C(Me)=NNMe_2)_2]_2$ and $Zn(CH_2C(Me)=NNMe_2)_2$, the methylene resonances appearing in the region 1–1.5 ppm were integrated for comparison with the integrated resonance of trichlorobenzene. Each equilibrium constant value was taken as the average of three separate integrations. A plot of $\ln K_{eq}$ versus $1/T$ yielded ΔH° and ΔS° . The errors in ΔH° and ΔS° were estimated from a linear regression analysis.

Single Crystal X-ray Diffraction Studies. All measurements were made with a Siemens SMART platform diffractometer equipped with a CCD area detector. The programs used in the X-ray diffraction studies were as follows: Data collection, Siemens APEX2 v1.0–27 (Bruker-Nonius, 2005); cell refinement and data reduction, Bruker SAINT v7.12A (Bruker-Nonius, 2004); structure solution, SHELXS v6.12 (G. M. Sheldrick, 2001); and structure refinement, SHELXL v6.12 (G. M. Sheldrick, 2001). The crystals of $[Li(CH_2C(i-Pr)=NNMe_2)(THF)]_n$ were colorless blocks; $[ClZn(CH_2C(Me)=NNMe_2)(py)]_2$ were very pale gold, multifaceted blocks; $[ClZn(CH_2C(t-Bu)=NNMe_2)]_2$ and $[Zn(CH_2C(Me)=NNMe_2)_2]_2$ were colorless, flat columns; $Zn(CH_2C(t-Bu)=NNMe_2)_2$ were colorless, diamond-shaped columns; and $[EtZn(CH_2C(Me)=NNMe_2)]_n$ were colorless plates. Crystal data are presented in Table 1.

In the crystal of $[Li(CH_2C(i-Pr)=NNMe_2)(THF)]_n$, the atoms in the asymmetric unit were found to be disordered. Two major orientations were found for the anion, and three major orientations for the THF. Attempts were made to model the disorder in the anion; however, this led to unreasonable bonding geometries and/or poor displacement parameters. Consequently, in the final refinement, only the isopropyl group was split and the remaining atoms in the anion were refined in single locations, allowing the anisotropic displacement parameters to absorb most of the positional disorder. In the $[ClZn(CH_2C(t-Bu)=NNMe_2)]_2$ crystal, the asymmetric unit consists of one molecule in a general position, and two half-molecules located on inversion centers. The geometric parameters of the three crystallographically independent molecules are essentially the same.

Results and Discussion

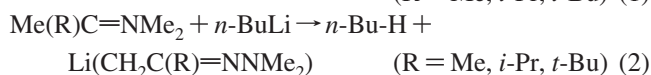
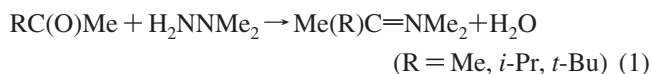
Synthesis of Ligand Precursors. The hydrazonide ligand precursors were lithium salts of the hydrazones, $Li(CH_2C(R)=NNMe_2)$. The salts were synthesized straightforwardly by deprotonating the dry hydrazones with n -BuLi (eqs 1 and 2).⁵ In the syntheses of $Me(i-Pr)C=NNMe_2$ and $Me(t-Bu)C=NNMe_2$ (eq 1), which were based on literature procedures,^{6–8} excess 1,1-dimethylhydrazine was used to

Table 1. Crystal Data for $[\text{Li}(\text{CH}_2\text{C}(i\text{-Pr})=\text{NNMe}_2)(\text{THF})]_n$, $[\text{ClZn}(\text{CH}_2\text{C}(\text{Me})=\text{NNMe}_2)(\text{py})]_2$, $[\text{ClZn}(\text{CH}_2\text{C}(t\text{-Bu})=\text{NNMe}_2)]_2$, $[\text{Zn}(\text{CH}_2\text{C}(\text{Me})=\text{NNMe}_2)_2]_2$, $\text{Zn}(\text{CH}_2\text{C}(t\text{-Bu})=\text{NNMe}_2)_2$, and $[\text{EtZn}(\text{CH}_2\text{C}(\text{Me})=\text{NNMe}_2)]_n$

chem formula	$\text{C}_{11}\text{H}_{23}\text{LiN}_2\text{O}$	$\text{C}_{20}\text{H}_{32}\text{N}_6\text{Cl}_2\text{Zn}_2$	$\text{C}_{16}\text{H}_{34}\text{N}_4\text{Cl}_2\text{Zn}_2$	$\text{C}_{20}\text{H}_{44}\text{N}_8\text{Zn}_2$	$\text{C}_{16}\text{H}_{34}\text{N}_4\text{Zn}$	$\text{C}_7\text{H}_{16}\text{N}_2\text{Zn}$
fw (g mol ⁻¹)	206.25	558.16	484.11	527.37	347.84	558.16
cryst dimens, mm	0.20 × 0.15 × 0.10	0.25 × 0.15 × 0.10	0.25 × 0.15 × 0.12	0.40 × 0.20 × 0.08	0.40 × 0.15 × 0.15	0.20 × 0.15 × 0.10
space group	<i>I</i> 2/a (monoclinic)	<i>P</i> bca (orthorhombic)	<i>P</i> 2 ₁ / <i>c</i> (monoclinic)	<i>P</i> 2 ₁ (monoclinic)	<i>P</i> $\bar{1}$ (triclinic)	<i>P</i> 2 ₁ / <i>c</i> (monoclinic)
<i>a</i> , Å	16.998(2)	13.2499(8)	11.6937	11.0006(5)	8.9360(6)	7.3601(5)
<i>b</i> , Å	9.1789(9)	18.3951(10)	17.8063(10)	8.8851(4)	9.6365(6)	12.9523(9)
<i>c</i> , Å	17.351(2)	20.4180(11)	21.9518(13)	14.2221(7)	12.6608(9)	9.4726(7)
α , deg	90	90	90	90	74.747(1)	90
β , deg	101.381(3)	90	97.942(1)	100.342(1)	70.743(1)	94.929(1)
γ , deg	90	90	90	90	86.822(1)	90
temp, K	223(2)	223(2)	223(2)	223(2)	223(2)	223(2)
<i>Z</i>	8	8	8	2	2	4
<i>V</i> , Å ³	2654.0(5)	4976.5(5)	4527.0(5)	1367.50(11)	992.40(12)	899.69(11)
<i>D</i> _{calcd} , g cm ⁻³	1.032	1.490	1.421	1.281	1.164	1.429
$\mu(\text{Mo K}\alpha)$, mm ⁻¹	0.065	2.161	2.361	1.775	1.238	2.663
<i>R</i> , <i>R</i> _w ^a	0.0753, 0.1960 ^b	0.0253, 0.0593 ^c	0.0229, 0.0508 ^d	0.0180, 0.0470 ^e	0.0276, 0.0716 ^f	0.0248, 0.0665 ^g

^a $R = \sum ||F_o| - |F_c|| / \sum |F_o|$; $R_w = [\sum w(F_o^2 - F_c^2)^2 / \sum w(F_o^2)^2]^{1/2}$. ^b $w = [\sigma^2(F_o^2) + (0.0995P)^2 + (0.0485P)]^{-1}$ where $P = (F_o^2 + 2F_c^2)/3$. ^c $w = [\sigma^2(F_o^2) + (0.0356P)^2 + (0.2700P)]^{-1}$. ^d $w = [\sigma^2(F_o^2) + (0.0276P)^2 + (0.0174)]^{-1}$. ^e $w = [\sigma^2(F_o^2) + (0.0326P)^2 + (0.000P)]^{-1}$. ^f $w = [\sigma^2(F_o^2) + (0.0480P)^2 + (0.0115P)]^{-1}$. ^g $w = [\sigma^2(F_o^2) + (0.0407P)^2 + (0.5225P)]^{-1}$.

minimize the amount of unreacted ketones in the product mixtures because the unreacted ketones have boiling points comparable to the respective hydrazones. The ¹H NMR spectrum of Me(*i*-Pr)C=NNMe₂ revealed a 90:10 *E*:*Z* isomeric ratio, but only one isomer was observed for the more sterically encumbered derivative Me(*t*-Bu)C=NNMe₂.



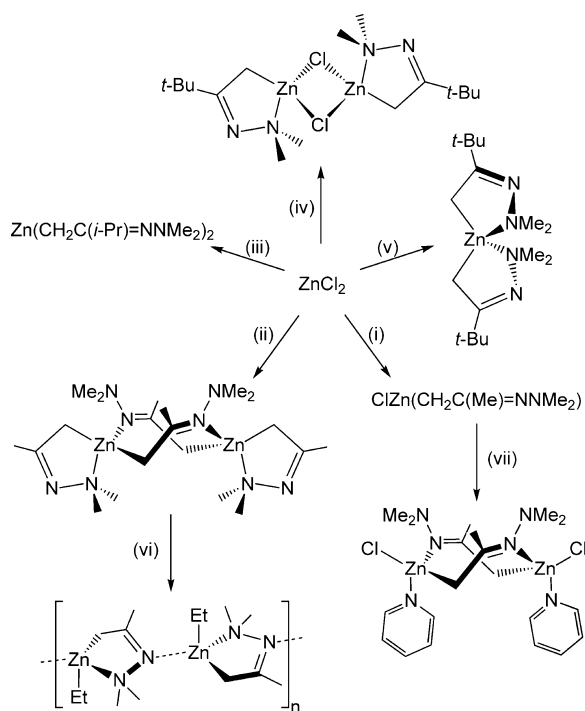
The lithium salts Li(CH₂C(Me)=NNMe₂), Li(CH₂C(*i*-Pr)=NNMe₂), and Li(CH₂C(*t*-Bu)=NNMe₂) were insoluble in diethyl ether and hydrocarbon solvents. The derivative Li(CH₂C(*i*-Pr)=NNMe₂) was crystallized from a THF solution for a single crystal X-ray diffraction analysis, but attempts to crystallize Li(CH₂C(Me)=NNMe₂) and Li(CH₂C(*t*-Bu)=NNMe₂) from THF solutions and by using other solvents were unsuccessful.

Synthesis of Zinc Hydrazone Complexes. A summary of our synthetic results is presented in Scheme 1.

To synthesize chlorido derivatives, ZnCl₂ was mixed in diethyl ether with 1 equiv of Li(CH₂C(R)=NNMe₂) to yield ClZn(CH₂C(R)=NNMe₂) where R = Me and *t*-Bu. The complex ClZn(CH₂C(*t*-Bu)=NNMe₂) was isolated in moderate yield as the hydrocarbon soluble dimer [ClZn(CH₂C(*t*-Bu)=NNMe₂)]₂. In the case of R = Me, a compound thought to be ClZn(CH₂C(Me)=NNMe₂) was isolated as a hydrocarbon-insoluble white powder. Because of its insolubility, ClZn(CH₂C(Me)=NNMe₂) was not characterized; instead, it was reacted with excess pyridine to yield the THF-soluble, monopyridine adduct [ClZn(CH₂C(Me)=NNMe₂)(py)]₂.

The synthesis of the homoleptic zinc complexes Zn(CH₂C(R)=NNMe₂)₂ where R = Me, *i*-Pr, or *t*-Bu was accomplished by allowing ZnCl₂ to react with 2 equiv of Li(CH₂C(R)=NNMe₂). The Zn(CH₂C(R)=NNMe₂)₂ complexes were crystallized from toluene, and as an additional purification step, all three derivatives could be sublimed cleanly at low temperatures (<75 °C at 0.01 mmHg).

In an attempt to prepare alkyl zinc hydrazone derivatives, ClZn(CH₂C(Me)=NNMe₂) was reacted with LiMe and LiEt

Scheme 1


at room temperature. According to ¹H NMR spectra, the desired alkyl complexes were minor components of the product mixtures. Attempts to isolate the alkyl complexes from the mixtures by fractional crystallization were unsuccessful.

An ethyl zinc hydrazone complex was eventually synthesized by allowing Zn(CH₂C(Me)=NNMe₂)₂ to react with excess ZnEt₂. The product, [EtZn(CH₂C(Me)=NNMe₂)]_n, is insoluble in hydrocarbon solvents; crystals suitable for a single crystal X-ray diffraction study were grown from a 1:1 mixture of THF and pentane. In contrast to these results, no reaction was observed when Zn(CH₂C(*t*-Bu)=NNMe₂)₂ was mixed with excess ZnEt₂.

Reactions with Ethylene. Our interest in zinc hydrazone complexes was aroused by the work of Nakamura et al., who described Zn–C insertion reactions involving proposed zinc hydrazone intermediates and olefinic substrates.^{1–3} With this in mind, we treated hydrocarbon solutions of [Zn–

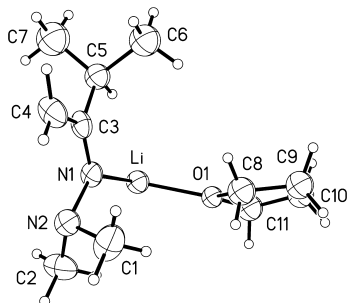


Figure 1. View of a piece of the $[\text{Li}(\text{CH}_2\text{C}(i\text{-Pr})=\text{NNMe}_2)(\text{THF})]_n$ polymer showing the atom-numbering scheme. Thermal ellipsoids are 40% equiprobability envelopes, with hydrogen atoms as spheres of arbitrary diameter. Only one orientation of each disordered group is shown.

$(\text{CH}_2\text{C}(\text{Me})=\text{NNMe}_2)_2$, $\text{Zn}(\text{CH}_2\text{C}(i\text{-Pr})=\text{NNMe}_2)_2$, and $\text{Zn}(\text{CH}_2\text{C}(t\text{-Bu})=\text{NNMe}_2)_2$, and THF solutions of $[\text{EtZn}(\text{CH}_2\text{C}(\text{Me})=\text{NNMe}_2)]_n$ with excess ethylene at atmospheric pressure and subjected these to moderate pressures of ethylene (up to 100 psi). In no case did a reaction occur as judged by examining ^1H NMR spectra of the product mixtures. The homoleptic zinc hydrazonide complexes did react, however, with nitriles via $\text{Zn}-\text{C}$ insertion to form β -diiminate complexes, and also with alkynes, ketones, and other unsaturated organic substrates. These studies are in progress and will be reported separately.

In those cases in which Nakamura et al. observed ethylene insertion, the proposed zinc hydrazonide intermediates were *n*-butyl derivatives of the type *n*-BuZn(hydrazonide). In contrast, three of the four complexes we attempted to react with ethylene were homoleptic hydrazonide complexes. The presence of the second hydrazonide with the potential to chelate through its imine or amine functional groups and thereby block ethylene access to zinc might be the reason the homoleptic complexes do not react with ethylene. Nitriles, which were found to react via insertion with the homoleptic zinc hydrazonide complexes, might have reacted because as stronger donors than ethylene, the nitriles might be able to coordinate to zinc when ethylene cannot. The polymeric ethyl complex $[\text{EtZn}(\text{CH}_2\text{C}(\text{Me})=\text{NNMe}_2)]_n$, which more closely resembles *n*-BuZn(hydrazonide), also did not react with ethylene, but in this case we found it necessary to use THF as the solvent because of the polymer insolubility in hydrocarbons. It is possible THF coordination to zinc blocked ethylene access to zinc and thereby precluded insertion of ethylene.

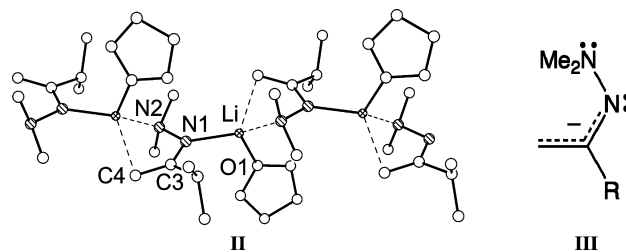
Solid-State Structures. The compounds $\text{Li}(\text{CH}_2\text{C}(i\text{-Pr})=\text{NNMe}_2)(\text{THF})$, $[\text{ClZn}(\text{CH}_2\text{C}(\text{Me})=\text{NNMe}_2)(\text{py})]_2$, $[\text{Zn}(\text{CH}_2\text{C}(\text{Me})=\text{NNMe}_2)_2]_2$, $[\text{ClZn}(\text{CH}_2\text{C}(t\text{-Bu})=\text{NNMe}_2)]_2$, $\text{Zn}(\text{CH}_2\text{C}(t\text{-Bu})=\text{NNMe}_2)_2$, and $[\text{EtZn}(\text{CH}_2\text{C}(\text{Me})=\text{NNMe}_2)]_n$ were characterized by using single crystal X-ray diffraction (Figures 1–6, respectively). Selected bond lengths and angles are presented in Tables 2 and 3.

The lithium salt $\text{Li}(\text{CH}_2\text{C}(i\text{-Pr})=\text{NNMe}_2)$ crystallized from THF solvent as the polymeric THF adduct $[\text{Li}(\text{CH}_2\text{C}(i\text{-Pr})=\text{NNMe}_2)(\text{THF})]_n$ (**II**). The lithium cation is bound to the imine nitrogen ($\text{Li}-\text{N1} = 2.055(7)$ Å) of one hydrazonide, and amine nitrogen ($\text{Li}-\text{N2}' = 2.234(7)$ Å) and methylene carbon ($\text{Li}-\text{C4} = 2.331(8)$ Å) of the adjacent

Table 2. Selected Bond Lengths (Å) and Angles (deg) in $[\text{Li}(\text{CH}_2\text{C}(i\text{-Pr})=\text{NNMe}_2)(\text{THF})]_n$

Li–O1	1.974(9)
Li–N1	2.055(7)
Li'–N2	2.234(7)
Li'–C4	2.331(8)
Li'–C3	2.727(7)
N1–N2	1.467(4)
C3–C4	1.365(5)
N1–C3	1.344(4)
O1–Li–N1	110.6(3)
O1–Li–N2'	110.8(3)
N1–Li–N2'	127.5(3)
O1–Li–C4'	111.7(3)
N1–Li–C4'	117.6(3)
N2'–Li–C4'	73.7(2)
O1–Li–C3'	95.4(3)
N1–Li–C3'	146.8(3)
N2'–Li–C3'	54.5(2)
C4'–Li–C3'	30.0(2)
C3–N1–N2	110.7(3)
C3–N1–Li	124.2(3)
N2–N1–Li	124.8(3)
N1–C3–C4	128.9(4)

hydrazonide. There is also a short contact between lithium and C3 ($\text{Li}-\text{C3} = 2.727(7)$ Å). These distances can be compared to those found in $\text{Li}(\text{CH}_2\text{Ph})(\text{TMEDA})\cdot\text{THF}$, where $\text{Li}-\text{CH}_2 = 2.210(5)$ Å and the average $\text{Li}-\text{N}_{\text{amine}} = 2.148(5)$ Å.⁹ Within the hydrazonide ion, the C3–C4 and C3–N1 distances (1.365(5) and 1.344(4) Å, respectively) may be compared to common C=C, $\text{C}_{\text{sp}^2}-\text{N}$, and C=N distances (1.34, 1.38, and 1.28 Å).¹⁰ On the basis of this comparison, there is delocalization of the charge over C4, C3, and N1, as illustrated in **III**, but disorder in the structure makes this conclusion dubious. Alternatively, the anion might be described as a hydrazide (i.e., $^-\text{N}(\text{NMe}_2)(\text{C}(i\text{-Pr})=\text{CH}_2)$).



In the solid state, the dimers $[\text{ClZn}(\text{CH}_2\text{C}(\text{Me})=\text{NNMe}_2)(\text{py})]_2$ and $[\text{Zn}(\text{CH}_2\text{C}(\text{Me})=\text{NNMe}_2)_2]_2$ (Figures 2 and 3) share the common structural feature of having bridging hydrazonide ligands that are each bound to one zinc atom via the imine nitrogen and to the other zinc atom via the methylene carbon, thereby forming 8-membered rings. In the complexes with a terminal hydrazonide ligand, $[\text{Zn}(\text{CH}_2\text{C}(\text{Me})=\text{NNMe}_2)_2]_2$, $[\text{ClZn}(\text{CH}_2\text{C}(t\text{-Bu})=\text{NNMe}_2)]_2$, $\text{Zn}(\text{CH}_2\text{C}(t\text{-Bu})=\text{NNMe}_2)_2$, and $[\text{EtZn}(\text{CH}_2\text{C}(\text{Me})=\text{NNMe}_2)]_n$ (Figures 3–6), the hydrazonide ligand is chelated to zinc through the methylene carbon and amine nitrogen, forming a 5-membered ring. The alkyl zinc hydrazonide complex $[\text{EtZn}(\text{CH}_2\text{C}(\text{Me})=\text{NNMe}_2)]_n$ (Figure 6) is a linear coordination polymer in the solid state wherein the polymerization occurs

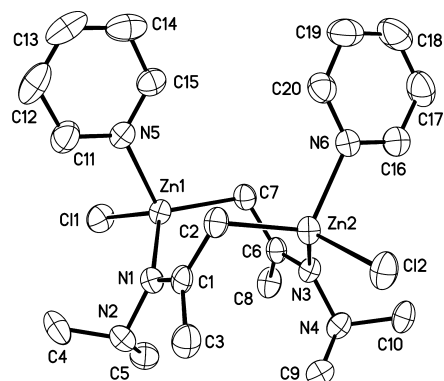
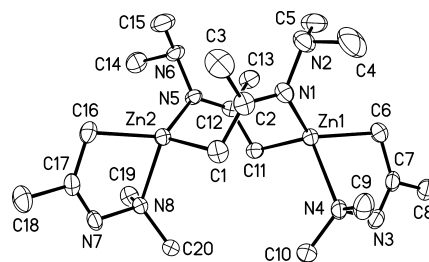
(9) Zarges, W.; Marsch, M.; Harms, K.; Boche, G. *Chem. Ber.* **1989**, *122*, 2303.

(10) Smith, M. B.; March, J. *Advanced Organic Chemistry*, 5th ed.; John Wiley & Sons: New York, 2001; p 20.

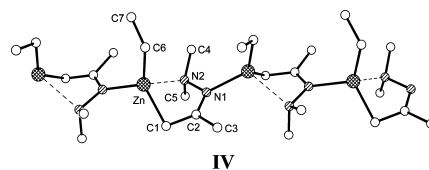
Table 3. Selected Bond Lengths (Å) and Angles (deg) in [ClZn(CH₂C(Me)=NNMe₂)(py)]₂, [Zn(CH₂C(Me)=NNMe₂)(py)]₂, [ClZn(CH₂C(*t*-Bu)=NNMe₂)]₂, [ClZn(CH₂C(*r*-Bu)=NNMe₂)]₂, Zn(CH₂C(*r*-Bu)=NNMe₂)₂, Zn(CH₂C(*r*-Bu)=NNMe₂)₂, and [EtZn(CH₂C(CH₃)=NNMe₂)]_n

	[ClZn(CH ₂ C(Me)=NNMe ₂)(py)] ₂	[Zn(CH ₂ C(Me)=NNMe ₂) ₂]	[ClZn(CH ₂ C(<i>r</i> -Bu)=NNMe ₂)] ₂	Zn(CH ₂ C(<i>r</i> -Bu)=NNMe ₂) ₂	[EtZn(CH ₂ C(Me)=NNMe ₂)] _n
Zn–C ^a	2.060(3), 2.058(3)	2.074(3), 2.083(2)	1.980(3), 1.982(3)	1.995(2), 1.997(2)	2.086(3)
Zn–C ^b		2.027(2), 2.023(2)			2.116(2)
Zn–N _{imine}	2.056(3), 2.059(3)	2.076(2), 2.068(2)	2.125(2), 2.141(2)	2.200(2), 2.203(2)	2.438(2)
Zn–N _{amine}	2.275(1), 2.272(1)	2.225(2), 2.246(2)	2.341(8) ^c		1.988(3) (X = C (Et))
Zn–X	(X = Cl)		(2.325(1)–2.346(1)) ^d		
C–N _{imine} ^a	1.304(4), 1.306(4)	1.303(3), 1.308(3)	1.280(3), 1.285(3)	1.286(3), 1.283(3)	1.310(4)
C–N _{amine} ^b		1.289(3), 1.280(3)			1.437(4)
C–CH ₂ ^a	1.441(4), 1.442(4)	1.437(3), 1.436(3)	1.498(3), 1.495(3)	1.485(3), 1.492(3)	1.458(3)
C–CH ₂ ^b		1.473(3), 1.471(3)	1.474(3), 1.470(3)	1.470(2), 1.475(2)	1.19.2(2)
N–N	1.455(3), 1.452(3)	1.462(3), ^c (1.456(3)–1.471(2)) ^d			1.28.4(2)
Zn–N _{imine} –N _{amine}	123.5(2), 122.5(2)	122.6(1), 121.1(1)			114.16(8)
Zn–N _{imine} –C	121.3(2), 121.3(2)	124.1(1), 123.8(2)			112.0(2)
N _{amine} –Zn–N _{imine}	114.7(3), 115.2(3)	108.7(1), 111.4(1)	113.9(2)	112.7(2), 112.5(2)	
C–N _{imine} –N _{amine}		113.5(2), ^c (113.1(2)–114.6(2)) ^d			

^a Bridging hydrazonide ligand. ^b Terminal hydrazonide ligand. ^c Average value. ^d Range of values.


Figure 2. View of [ClZn(CH₂C(Me)=NNMe₂)(py)]₂ showing the atom-numbering scheme. Thermal ellipsoids are 40% equiprobability envelopes, with hydrogen atoms omitted.

Figure 3. View of [Zn(CH₂C(Me)=NNMe₂)₂]₂ showing the atom-numbering scheme. Thermal ellipsoids are 40% equiprobability envelopes, with hydrogen atoms omitted.

via interaction of the zinc with the imine nitrogen (Zn–N1' = 2.116(2) Å) on the adjacent hydrazonide ligand (**IV**).

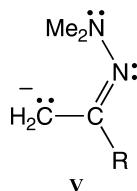


The zinc complexes have 4-coordinate zinc atoms, and collectively there is a wide variation in the angles about zinc (72°–154°). The smallest angles are the bite angles of the terminal chelating hydrazonide ligands, and the largest angles are the H₂C–Zn–CH₂ angles in [Zn(CH₂C(Me)=NNMe₂)₂]₂, Zn(CH₂C(*t*-Bu)=NNMe₂)₂, and [EtZn(CH₂C(Me)=NNMe₂)]_n. In the monomer Zn(CH₂C(*t*-Bu)=NNMe₂)₂, the H₂C–Zn–CH₂ angle is 154°, and the zinc has a distorted seesaw coordination geometry that closely resembles the known complex Zn[(CH₂)₃NMe₂]₂.¹¹ The geometries about zinc in the other structures are not easily defined, but zinc may be described loosely as trigonal pyramidal in [ClZn(CH₂C(*t*-Bu)=NNMe₂)]₂ (apical group = NMe₂), [Zn(CH₂C(Me)=NNMe₂)₂]₂ (apical group = NMe₂), and [EtZn(CH₂C(Me)=NNMe₂)]_n (apical group = Et), where the sum of the basal plane X–Zn–Y angles in each case is about 354°.

Within the hydrazonide ligands, the bridging hydrazonide C–CH₂Zn distances (av. 1.439(4) Å) are slightly shorter than the terminal hydrazonide C–CH₂Zn distances (av. 1.486(3) Å), except in the polymer [EtZn(CH₂C(Me)=NNMe₂)]_n.

(11) Dekker, J.; Boersma, J.; Fernholt, L.; Haaland, A.; Spek, A. L. *Organometallics* **1987**, *6*, 1202.

where the terminal hydrazone C–CH₂Zn distance is 1.437(4) Å. Similarly, the bridging hydrazone C–N_{imine} distances (av. 1.305(4) Å) are slightly longer than the terminal hydrazone C–N_{imine} distances (av. 1.284(3) Å), except in the polymer [EtZn(CH₂C(Me)=NNMe₂)]_n where C–N_{imine} = 1.310(4) Å. The C–CH₂Zn distances may be compared to the normal distances for C=C, C_{sp2}–C_{sp2}, and C_{sp2}–C_{sp3} bonds (1.34, 1.48, and 1.50 Å, respectively),¹⁰ and the C–N_{imine} distances may be compared to the normal distances for C=N and C_{sp2}–N (1.28 and 1.36 Å, respectively).¹⁰ The distances within the bridging hydrazones in [ClZn(CH₂C(Me)=NNMe₂)(py)]₂ and [Zn(CH₂C(Me)=NNMe₂)₂]₂ also contrast with the distances found in three palladacycles incorporating terminal chelating hydrazone ligands, the only other structurally characterized hydrazone complexes.^{12–14} In the palladacycles, the C–CH₂Pd and C–N_{imine} distances average 1.51 and 1.28 Å, respectively,^{12–14} indicating localization of the charge on the hydrazone methylene carbon as described by **V**.



On the basis of the bond lengths in [ClZn(CH₂C(Me)=NNMe₂)(py)]₂, [Zn(CH₂C(Me)=NNMe₂)₂]₂, [ClZn(CH₂C(*t*-Bu)=NNMe₂)₂], and Zn(CH₂C(*t*-Bu)=NNMe₂)₂, and comparisons to the known palladacycles, there is more delocalization of the charge in the bridging hydrazone ligands, as described by **III**, than in the terminal hydrazone ligands, where **V** is the predominant contributor. As explained below, there is also NMR evidence for three-center charge delocalization in the bridging hydrazone ligands of [Zn(CH₂C(Me)=NNMe₂)₂]₂ and [ClZn(CH₂C(Me)=NNMe₂)(py)]₂. The shortened C–CH₂ distance and elongated C–N_{imine} distance in the polymer [EtZn(CH₂C(CH₃)=NNMe₂)]_n suggest there is also charge delocalization in its hydrazone ligand.

The hydrazone Zn–CH₂ distances in [ClZn(CH₂C(Me)=NNMe₂)(py)]₂ (av. 2.059(3) Å), [Zn(CH₂C(Me)=NNMe₂)₂]₂ (av. 2.079(3) Å), [ClZn(CH₂C(*t*-Bu)=NNMe₂)₂] (av. 1.981(3) Å), Zn(CH₂C(*t*-Bu)=NNMe₂)₂ (av. 1.996(2) Å), and [EtZn(CH₂C(Me)=NNMe₂)]_n (2.086(3) Å) may be compared, for example, to the Zn–C distances in Zn[(CH₂)₃NMe₂]₂ (1.984(5) Å),¹¹ Zn(*t*-Bu)₂ (1.977(4) Å),¹⁵ [Zn(*t*-Bu)₂(1,2-bis(4-pyridyl)ethane)]_n (av. 2.035(3) Å),¹⁵ Zn[C(SiMe₃)₂]₂ (av. 1.982(2) Å),¹⁶ and [EtZn(NHNMe₂)₄] (av. 2.013(6) Å).¹⁷

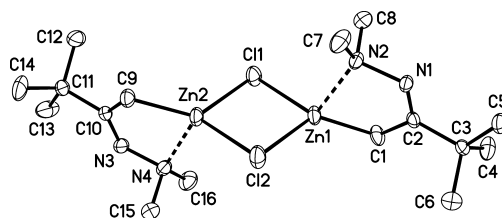


Figure 4. View of [ClZn(CH₂C(*t*-Bu)=NNMe₂)]₂ showing the atom-numbering scheme. Thermal ellipsoids are 40% equiprobability envelopes, with hydrogen atoms omitted.

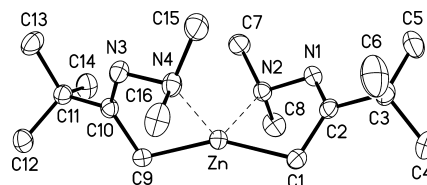


Figure 5. View of Zn(CH₂C(*t*-Bu)=NNMe₂)₂ showing the atom-numbering scheme. Thermal ellipsoids are 40% equiprobability envelopes, with hydrogen atoms omitted.

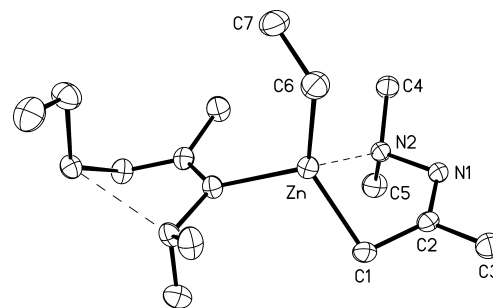


Figure 6. View of a piece of the [EtZn(CH₂C(Me)=NNMe₂)]_n polymer showing the atom-numbering scheme. Thermal ellipsoids are 40% equiprobability envelopes, with hydrogen atoms omitted.

Similarly, the Zn–N_{amine} and Zn–N_{imine} distances in [ClZn(CH₂C(Me)=NNMe₂)(py)]₂ (Zn–N_{imine} av. 2.058(3) Å), [Zn(CH₂C(Me)=NNMe₂)₂]₂ (Zn–N_{amine} av. 2.235(2) Å; Zn–N_{imine} av. 2.072(2) Å), [ClZn(CH₂C(*t*-Bu)=NNMe₂)₂] (Zn–N_{amine} av. 2.133(2) Å), Zn(CH₂C(*t*-Bu)=NNMe₂)₂ (Zn–N_{amine} av. 2.202(2) Å), and [EtZn(CH₂C(Me)=NNMe₂)]_n (Zn–N_{amine} = 2.438(2) Å; Zn–N_{imine} = 2.116(2)) may be compared to the Zn–N_{amine/imine} distances found in Zn[(CH₂)₃NMe₂]₂ (2.307(4) Å),¹¹ ZnMe₂[cyclo-(CH₂NMe₂)₃]₂ (2.410(4) Å),¹⁸ ZnEt₂(Et₂NCH₂CH₂NEt₂) (av. 2.263(2) Å),¹⁹ Zn(O-2,6-*t*-Bu₂C₆H₃)Me(Me₂NC(N-*i*-Pr)(NH-*i*-Pr)) (1.995(2) Å),²⁰ [ZnMe(O₂CNR₂)(py)]₂ (R = *i*-Pr and *i*-Bu, av. 2.121(2) Å),²¹ ZnMe₂(py-*p*-NMe₂)₂ (av. 2.023(2) Å)²² and [Zn(*t*-Bu)₂(1,2-bis(4-pyridyl)ethane)]_n (2.220(3) Å).¹⁵

NMR Characterization. In the solid state, the dimer [ClZn(CH₂C(*t*-Bu)=NNMe₂)]₂ has virtual C_{2h} symmetry (Figure 4). The ¹H NMR spectrum of [ClZn(CH₂C(*t*-Bu)=NNMe₂)]₂ at room temperature is consistent with the

(12) Galli, B.; Gasparrini, F.; Mann, B. E.; Maresca, L.; Natile, G.; Manotti-Lanfredi, A. M.; Tiripicchio, A. *J. Chem. Soc., Dalton Trans.* **1985**, 1155.
 (13) Cárdenas, D. J.; Echavarren, A. M.; Vegas, A. *Organometallics* **1994**, *13*, 882.
 (14) Constable, A. G.; McDonald, W. S.; Sawkins, L. C.; Shaw, B. L. *J. Chem. Soc., Dalton Trans.* **1980**, 1992.
 (15) Lewinski, J.; Dranka, M.; Bury, W.; Sliwinski, W.; Iwona, J.; Lipkowski, J. *J. Am. Chem. Soc.* **2007**, *129*, 3096.
 (16) Westerhausen, M.; Rademacher, B.; Poll, W. *J. Organomet. Chem.* **1991**, *421*, 175.

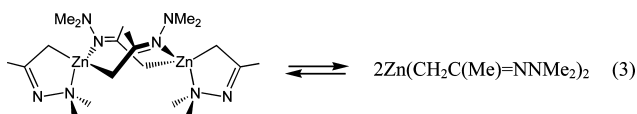
(17) Jana, S.; Fröhlich, R.; Mitzel, N. W. *Chem.—Eur. J.* **2006**, *12*, 592.
 (18) Hursthouse, M. B.; Motevalli, M.; O'Brien, P.; Walsh, J. R. *Organometallics* **1991**, *10*, 3196.
 (19) Johansson, A.; Wingstrand, E.; Håkansson, M. *J. Organomet. Chem.* **2005**, *690*, 3846.
 (20) Coles, M. P.; Hitchcock, P. B. *Eur. J. Inorg. Chem.* **2004**, 2662.
 (21) Tang, Y.; Kassel, W. S.; Zakharov, L. N.; Rheingold, A. L.; Kemp, R. A. *Inorg. Chem.* **2005**, *44*, 359.
 (22) Thomas, F.; Schultz, S.; Nieger, M. *Angew. Chem., Int. Ed.* **2005**, *44*, 5668.

solid state structure, showing singlet resonances in the methylene, methyl, and amine methyl regions with relative intensities 2:9:6, respectively.

The homoleptic dimer $[\text{Zn}(\text{CH}_2\text{C}(\text{Me})=\text{NNMe}_2)_2]_2$ has virtual C_2 symmetry in the solid state with two terminal and two bridging hydrazone ligands (Figure 3). Consistent with this, the ^1H NMR spectrum recorded at room temperature revealed two CH_2 AB quartets, two CMe singlets, two NMe_2 singlets, and a broad NMe_2 resonance. The broad NMe_2 resonance is reasonably assigned to the bridging hydrazone ligand; the NMe_2 groups of the bridging hydrazone ligands are expected to invert rapidly at nitrogen concomitant with N–N bond rotation to interchange the two methyl groups. Consistent with this interpretation, the ^1H NMR spectrum recorded at -80°C (toluene- d_8) resolves the broad NMe_2 resonance into two singlets.

In the ^1H NMR spectra of $[\text{Zn}(\text{CH}_2\text{C}(\text{Me})=\text{NNMe}_2)_2]_2$, the methylene AB quartet assigned to the bridging hydrazone ligand is shifted unusually downfield and has a small gem-CH_2 coupling constant, whereas the chemical shifts and coupling constant for the terminal hydrazone methylene AB quartet are normal (cf. 1.77 and 2.27 ppm with $^2J_{\text{HH}} = 4$ Hz for the bridging hydrazone ligand vs 1.33 and 1.38 ppm with $^2J_{\text{HH}} = 13$ Hz for the terminal hydrazone ligand). Similarly, the ^{13}C – ^1H COSY spectrum showed that the ^{13}C chemical shift of the methylene carbon resonance arising from the bridging hydrazone ligand was 10 ppm downfield from the methylene carbon resonance of the terminal hydrazone ligand. These data suggest that the methylene group of the bridging hydrazone ligand has sp^2 character (i.e., sp^2 gem-CH_2 coupling is typically -3 to 7 Hz, while sp^3 gem-CH_2 coupling is typically -10 to -18 Hz).²³ The spectroscopic data are also consistent with the structural data from the single crystal X-ray diffraction study that suggested charge delocalization in the bridging hydrazone ligand (see above).

Interestingly, the room temperature ^1H NMR spectrum of $[\text{Zn}(\text{CH}_2\text{C}(\text{Me})=\text{NNMe}_2)_2]_2$ also contained singlet resonances in the methylene, methyl, and amine methyl regions that were consistent with the presence of the monomer $\text{Zn}(\text{CH}_2\text{C}(\text{Me})=\text{NNMe}_2)_2$ having a proposed structure analogous to $\text{Zn}(\text{CH}_2\text{C}(t\text{-Bu})=\text{NNMe}_2)_2$. A subsequent variable temperature ^1H NMR study (e.g., Figure 7) showed that the dimer and monomer were in equilibrium (eq 3). A van't Hoff plot gave $\Delta H^\circ = 55.8(2.9)$ kJ/mol, $\Delta S^\circ = 144(2)$ J/mol K, and $\Delta G^\circ_{298\text{K}} = 13(2)$ kJ/mol (Figure 8). The results indicate the dimer is thermodynamically favored at room temperature, and ΔS° is as expected for a dimer converting to two monomers.



The solid-state structure of $\text{Zn}(\text{CH}_2\text{C}(t\text{-Bu})=\text{NNMe}_2)_2$ has virtual C_2 symmetry (Figure 5). If this symmetry is main-

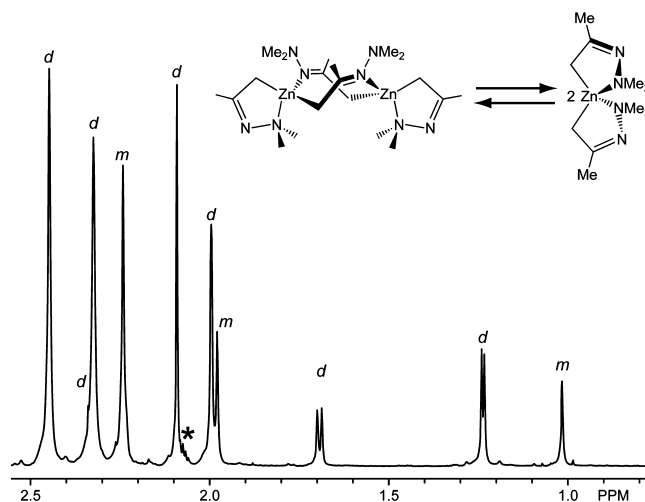


Figure 7. Proton NMR spectrum of $[\text{Zn}(\text{CH}_2\text{C}(\text{Me})=\text{NNMe}_2)_2]_2$ in toluene- d_8 at 55°C showing resonances consistent with a proposed dimer-monomer equilibrium (d = dimer; m = monomer). The resonance indicated with the * is a solvent resonance.

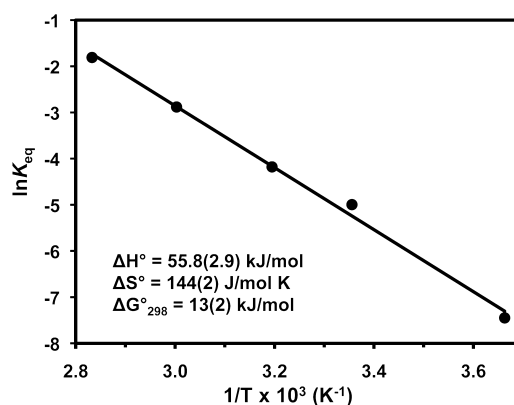


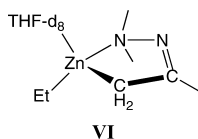
Figure 8. Van't Hoff plot for the dimer-monomer equilibrium $[\text{Zn}(\text{CH}_2\text{C}(\text{Me})=\text{NNMe}_2)_2]_2 \rightleftharpoons 2\text{Zn}(\text{CH}_2\text{C}(\text{Me})=\text{NNMe}_2)_2$.

tained in solution, the ^1H NMR spectrum should display an AB quartet in the methylene region, a singlet resonance in the $t\text{-Bu}$ region, and two singlets in the amine methyl region. At room temperature, the ^1H NMR spectrum consisted of three singlets in the methylene, amine methyl, and $t\text{-Bu}$ regions with relative intensities 2:6:9. The ^1H NMR spectrum recorded for a toluene- d_8 solution at -70°C was not significantly different from the room temperature spectrum. These data are consistent with a low energy fluxional process rendering the molecule with mirror symmetry. A mechanism involving Zn– N_{amine} bond rupture, Zn–C bond rotation, and Zn– N_{amine} bond reformation would accomplish this. Proton NMR spectra for $\text{Zn}(\text{CH}_2\text{C}(i\text{-Pr})=\text{NNMe}_2)_2$ were analogous to those observed for the $t\text{-Bu}$ complex.

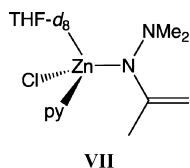
In the solid state, $[\text{EtZn}(\text{CH}_2\text{C}(\text{Me})=\text{NNMe}_2)]_n$ is a polymer (**IV**). The complex was not soluble in non-coordinating solvents. The ^1H NMR spectrum of a THF- d_8 solution of $[\text{EtZn}(\text{CH}_2\text{C}(\text{Me})=\text{NNMe}_2)]_n$ consisted of three singlets in the methylene, methyl, and amine methyl regions with relative intensities 2:3:6, suggesting that the coordinating solvent cleaved the polymer. Chemical shifts and coupling constants were consistent with a terminal chelating hydrazone ligand, as in $[\text{ClZn}(\text{CH}_2\text{C}(t\text{-Bu})=\text{NNMe}_2)]_2$. A structure such as the one shown in **VI** is a possible explanation

(23) Abraham, R. J.; Fisher, J.; Loftus, P. *Introduction to NMR Spectroscopy*; John Wiley & Sons: New York, 1988; p 41.

for the data if there is rapid exchange of THF- d_8 coupled with planarization at Zn, or there is rapid Zn–N_{amine} bond rupture, planarization at Zn, and Zn–N_{amine} bond reformation.



Because of the structural similarity of the bridging hydrazonide ligands in $[\text{Zn}(\text{CH}_2\text{C}(\text{Me})=\text{NNMe}_2)_2]_2$ (Figure 3) and $[\text{ClZn}(\text{CH}_2\text{C}(\text{Me})=\text{NNMe}_2)(\text{py})]_2$ (Figure 2), we anticipated similar NMR spectra for the two compounds. The ^1H NMR spectrum for a THF- d_8 solution at room temperature revealed normal singlet resonances for the *CMe* and *NMe*₂ protons, and the methylene protons appeared as an AB quartet. The methylene proton resonances were shifted downfield by about 2 ppm from where they appeared for the bridging ligands in $[\text{Zn}(\text{CH}_2\text{C}(\text{Me})=\text{NNMe}_2)_2]_2$ and the two-bond coupling H–H constant was smaller ($J_{\text{HH}} = 1.5$ Hz vs 4 Hz). Interestingly, in the ^{13}C – ^1H COSY spectrum the methylene protons in $[\text{ClZn}(\text{CH}_2\text{C}(\text{Me})=\text{NNMe}_2)(\text{py})]_2$ correlated to a carbon-13 resonance at 95 ppm, which was far downfield from the carbon-13 resonance for the bridging hydrazonide methylene carbon in $[\text{Zn}(\text{CH}_2\text{C}(\text{Me})=\text{NNMe}_2)_2]_2$ (34 ppm). These data are consistent with considerable sp^2 character at the hydrazonide methylene carbon in $[\text{ClZn}(\text{CH}_2\text{C}(\text{Me})=\text{NNMe}_2)(\text{py})]_2$, suggesting substantial charge delocalization as depicted in **III**. Another possible explanation for the anomalous NMR data is that the hydrazonide ligand converted in solution to a bridging hydrazide ligand, $^-\text{N}(\text{NMe}_2)(\text{C}(\text{Me})=\text{CH}_2)$, or similarly, the coordinating solvent cleaved the dimer, producing a complex having a terminal hydrazide ligand (e.g., **VII**).



Conclusion

The zinc hydrazonide complexes $[\text{ClZn}(\text{CH}_2\text{C}(t\text{-Bu})=\text{NNMe}_2)_2]$, $[\text{ClZn}(\text{CH}_2\text{C}(\text{Me})=\text{NNMe}_2)(\text{py})]_2$, $[\text{Zn}(\text{CH}_2\text{C}(\text{Me})=\text{NNMe}_2)_2]_2$, $\text{Zn}(\text{CH}_2\text{C}(i\text{-Pr})=\text{NNMe}_2)_2$, and $\text{Zn}(\text{CH}_2\text{C}(t\text{-Bu})=\text{NNMe}_2)_2$ were synthesized by using salt metathesis

reactions, and the polymer $[\text{EtZn}(\text{CH}_2\text{C}(\text{Me})=\text{NNMe}_2)]_n$ was obtained by mixing excess ZnEt_2 with $[\text{Zn}(\text{CH}_2\text{C}(\text{Me})=\text{NNMe}_2)_2]_2$ at room temperature. Single crystal X-ray diffraction studies showed that the hydrazonide ligands are bound to zinc as chelating alkyl ligands. The hydrazonide ligand precursor $[\text{Li}(\text{CH}_2\text{C}(i\text{-Pr})=\text{NNMe}_2)(\text{THF})]_n$ was also isolated and its solid-state structure determined. In the anion of $[\text{Li}(\text{CH}_2\text{C}(i\text{-Pr})=\text{NNMe}_2)(\text{THF})]_n$, hydrazonide ligand in $[\text{EtZn}(\text{CH}_2\text{C}(\text{Me})=\text{NNMe}_2)]_n$, and bridging hydrazonide ligands in $[\text{Zn}(\text{CH}_2\text{C}(\text{Me})=\text{NNMe}_2)_2]_2$ and $[\text{ClZn}(\text{CH}_2\text{C}(\text{Me})=\text{NNMe}_2)(\text{py})]_2$, there is evidence for three-center charge delocalization. In solution, the dimer $[\text{Zn}(\text{CH}_2\text{C}(\text{Me})=\text{NNMe}_2)_2]_2$ is in equilibrium with the monomer $\text{Zn}(\text{CH}_2\text{C}(\text{Me})=\text{NNMe}_2)_2$ with the thermodynamic parameters $\Delta H^\circ = 55.8(2.9)$ kJ/mol, $\Delta S^\circ = 144(2)$ J/mol K, and $\Delta G^\circ_{298\text{K}} = 13(2)$ kJ/mol.

Solutions of $[\text{Zn}(\text{CH}_2\text{C}(\text{Me})=\text{NNMe}_2)_2]_2$, $\text{Zn}(\text{CH}_2\text{C}(i\text{-Pr})=\text{NNMe}_2)_2$, $\text{Zn}(\text{CH}_2\text{C}(t\text{-Bu})=\text{NNMe}_2)_2$, and $[\text{EtZn}(\text{CH}_2\text{C}(\text{Me})=\text{NNMe}_2)]_n$ did not react with ethylene at atmospheric and higher pressures (up to 100 psi). This is surprising given the results reported by Nakamura et al.,^{1–3} who observed under mild conditions ethylene insertion reactions into the Zn–C bonds of proposed zinc hydrazonide intermediates of the type $n\text{-BuZn}(\text{hydrazonide})$. The differences between the proposed zinc hydrazonide intermediates Nakamura et al. observed to react with ethylene and our complexes that failed to react with ethylene suggest alkyl derivatives, $\text{RZn}(\text{hydrazonide})$, with bulky alkyl and/or hydrazonide ligands might be better candidates for olefin insertion and polymerization activity than the hydrazonide complexes we have reported. Studies of other Zn–C insertion chemistry involving the homoleptic zinc hydrazonide complexes described in this paper are also in progress.

Acknowledgment. Dr. James Korp provided technical assistance with the crystal structure determinations. The Robert A. Welch Foundation (Grant E-1206) provided full support for this research.

Supporting Information Available: X-ray crystallographic data in CIF format for $\text{Li}(\text{CH}_2\text{C}(i\text{-Pr})=\text{NNMe}_2)(\text{THF})$, $[\text{ClZn}(\text{CH}_2\text{C}(\text{Me})=\text{NNMe}_2)(\text{py})]_2$, $[\text{Zn}(\text{CH}_2\text{C}(\text{Me})=\text{NNMe}_2)_2]_2$, $[\text{ClZn}(\text{CH}_2\text{C}(t\text{-Bu})=\text{NNMe}_2)]_2$, $\text{Zn}(\text{CH}_2\text{C}(t\text{-Bu})=\text{NNMe}_2)_2$, and $[\text{EtZn}(\text{CH}_2\text{C}(\text{Me})=\text{NNMe}_2)]_n$. This material is available free of charge via the Internet at <http://pubs.acs.org>.

IC801451V